

**Zeitschrift:** IABSE proceedings = Mémoires AIPC = IVBH Abhandlungen  
**Band:** 4 (1980)  
**Heft:** P-30: Fatigue resistant tendonds for cable-stayed construction  
  
**Artikel:** Fatigue resistant tendonds for cable-stayed construction  
**Autor:** Birkenmaier, M.  
**DOI:** <https://doi.org/10.5169/seals-34955>

### **Nutzungsbedingungen**

Die ETH-Bibliothek ist die Anbieterin der digitalisierten Zeitschriften auf E-Periodica. Sie besitzt keine Urheberrechte an den Zeitschriften und ist nicht verantwortlich für deren Inhalte. Die Rechte liegen in der Regel bei den Herausgebern beziehungsweise den externen Rechteinhabern. Das Veröffentlichen von Bildern in Print- und Online-Publikationen sowie auf Social Media-Kanälen oder Webseiten ist nur mit vorheriger Genehmigung der Rechteinhaber erlaubt. [Mehr erfahren](#)

### **Conditions d'utilisation**

L'ETH Library est le fournisseur des revues numérisées. Elle ne détient aucun droit d'auteur sur les revues et n'est pas responsable de leur contenu. En règle générale, les droits sont détenus par les éditeurs ou les détenteurs de droits externes. La reproduction d'images dans des publications imprimées ou en ligne ainsi que sur des canaux de médias sociaux ou des sites web n'est autorisée qu'avec l'accord préalable des détenteurs des droits. [En savoir plus](#)

### **Terms of use**

The ETH Library is the provider of the digitised journals. It does not own any copyrights to the journals and is not responsible for their content. The rights usually lie with the publishers or the external rights holders. Publishing images in print and online publications, as well as on social media channels or websites, is only permitted with the prior consent of the rights holders. [Find out more](#)

**Download PDF:** 22.08.2025

**ETH-Bibliothek Zürich, E-Periodica, <https://www.e-periodica.ch>**

## **Fatigue Resistant Tendons for Cable-Stayed Construction**

Câbles résistant à la fatigue pour les ouvrages haubannés

Ermüdungsfeste Zugglieder für Schrägseil-Konstruktionen

**M. BIRKENMAIER**

Dipl.-Ing. ETH, Dr. h.c.  
Bureau BBR Ltd.  
Zürich, Switzerland

### **SUMMARY**

The tendons in certain cable-stayed structures can be subjected to severe fatigue loading. This paper describes the development and construction of the DINA and HiAm parallel wire tendons with excellent fatigue resistance suitable for use in such structures.

A method of determining a safe value for the permissible stress range in large parallel wire tendons based on a series of systematic fatigue tests on the wire alone is also described.

### **RÉSUMÉ**

Les câbles de certaines constructions haubannées peuvent être soumis à des fatigues élevées. Cette publication décrit la conception de câbles à fils parallèles spéciaux (câbles DINA ou HiAm) qui ont une résistance à la fatigue très élevée.

Il est démontré sur la base d'essais systématiques sur des fils d'acier qu'on peut déduire des valeurs sûres pour la sollicitation admissible à la fatigue de grands câbles à fils parallèles.

### **ZUSAMMENFASSUNG**

Zugglieder in gewissen Schrägseil-Konstruktionen können hohen Ermüdungsbeanspruchungen ausgesetzt sein. Im vorliegenden Beitrag werden Aufbau und Wirkungsweise von speziellen Parallel-Drahtkabeln (sog. DINA- und HiAm-Kabeln) beschrieben, welche hervorragende Ermüdungsfestigkeiten aufweisen und daher für solche Schrägseil-Konstruktionen besonders geeignet sind.

Es wird gezeigt, wie aufgrund systematischer Ermüdungsversuche an Stahldrähten sichere Werte für die zulässige Ermüdungsbeanspruchung von grossen Parallel-Drahtkabeln gewonnen werden können.



## 1. INTRODUCTION

### 1.1 General

During recent years cable stayed construction has found increasing use in building and, above all, in bridge structures. In this form of construction the main girders are supported by inclined tendons tied back to the pylons. [1] The load behaviour and durability of this form of construction is strongly influenced by the type of tendon used. In certain types of projects the fatigue resistance properties of the tendons will be the decisive criterion in choosing tendon sizes.

### 1.2 Numerical example

The following numerical example illustrates some of the features encountered in the design of cable stayed structures. (Fig.1).

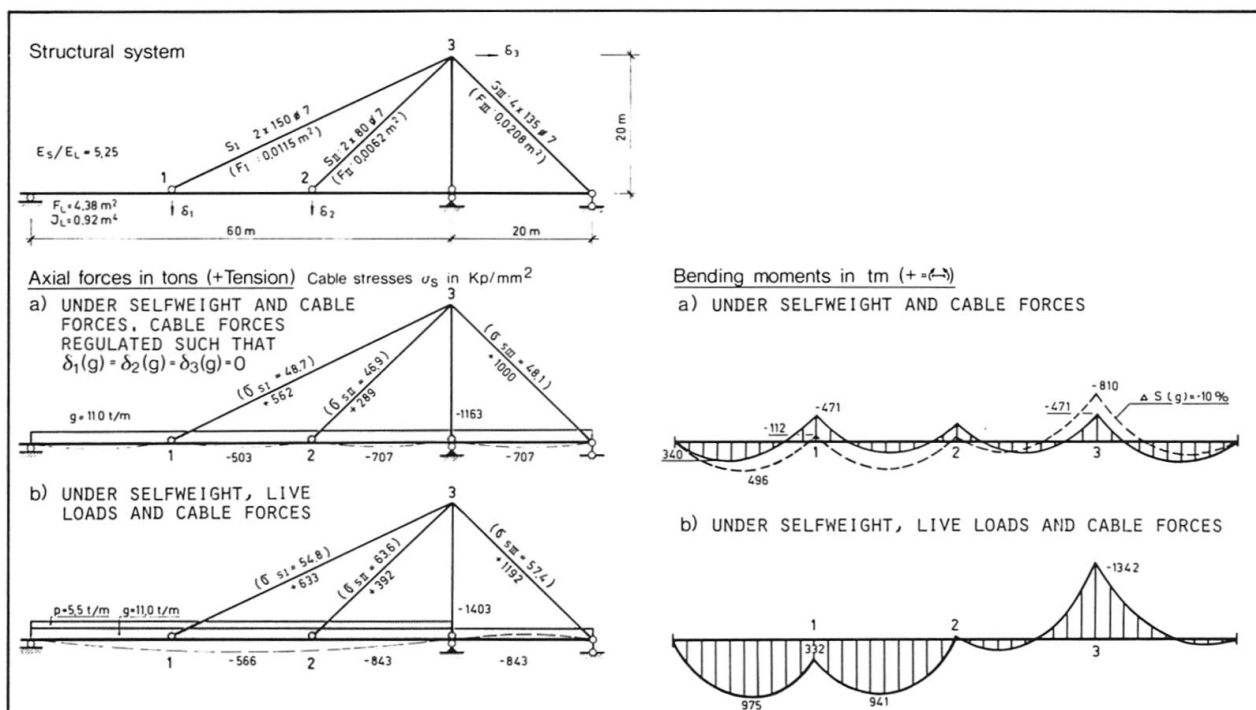


Fig.1

A two-span bridge girder with 60 and 20 m spans is supported by 3 inclined parallel wire tendons S<sub>I</sub>, S<sub>II</sub> and S<sub>III</sub> (S<sub>I</sub> = 2 x 150  $\phi$  7 mm; S<sub>II</sub> = 2 x 80  $\phi$  7 mm; S<sub>III</sub> = 4 x 135  $\phi$  7 mm). The stay cables are tied back to a vertical pylon at a height of 20 m above the bridge deck. This structural system is 3 times statically indeterminate. The initial forces in the stay cables are regulated to result in zero values for the deflections  $\delta_1$ ,  $\delta_2$  and  $\delta_3$  under the self weight loads of  $g = 11$  t/m. The bending moments  $M(g)$  in the bridge girder under self weight and the cable forces can be calculated as for a beam continuous over 4 supports. If the forces introduced initially in the stay cables are reduced by 10 % the resulting increase in bending moments at certain sections of the bridge girder can be considerable; for example the negative bending moment in the girder at the pylon support increases from 471 tm to 810 tm, an increase of 72 %. In cable stayed structures it is therefore very important that the required initial forces are introduced into the cables accurately, and that these forces act permanently during the life of the structure.

The distribution of the bending moments  $M(g+p)$  in the bridge girder under self weight, live loads and cable forces clearly shows the influence of the girder displacements  $\delta_1$  and  $\delta_2$  resulting from the elastic extensions of the inclined stay cables.

The pylon and bridge girder are subject to large compressive forces. These forces produce additional second order bending moments in the deformed structural system which in some cases should be included in the design. In most cases it will be sufficient to calculate these additional moments from the first order deformations of the structural system.


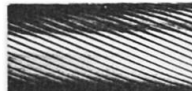
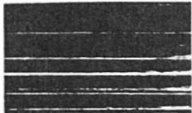
Under the action of the entire live load on the bridge the stress in cable  $S_{II}$  increases from  $46.9 \text{ kp/mm}^2$  to  $63.6 \text{ kp/mm}^2$ , i.e. an increase  $\Delta\sigma = 16.7 \text{ kp/mm}^2$ . The fluctuation of this stress increase subjects the stay cable and its anchorages to fatigue. It will be shown later that fatigue resistance of the tendons is very often a decisive design characteristic in cable stayed structures.

### 1.3 Types of stay cables

Fig.2 shows the three types of stay cables commonly used

- spiral strand rope
- locked coil rope
- parallel-wire or parallel-strand tendons

Fig.2

	SPIRAL STRAND	LOCKED COIL	PARALLEL WIRE
			
diameter max. mm	80	110	160
area max. $\text{cm}^2$	28	85	150
breaking force max. MN	5	13	26

These three types of cables differ considerably from one another in their load capacity, load behaviour and the anchorages employed with them.

The parallel-wire tendon will be referred to in the rest of this article.

## 2. PARALLEL-WIRE TENDONS

### 2.1 The wire bundle

Fig.3 shows a cross-section and cut-out elevation of a parallel wire tendon consisting of 163 wires 7 mm diameter (ultimate tensile load 1000 t). The wire bundle is enclosed by a polyethylene duct. A strand 10 mm dia. wound around the bundle acts as a spacer between the bundle and the duct. The wires in the bundle are coated with a film of anticorrosion fluid. After the final adjustment of the initial forces in the stay cables the duct is filled with an anti-corrosion medium. This generally consists of an epoxy enriched cement grout which is pumped into the duct by a suitable grout pump commencing at the lower end of the stay cable. The grouting should be carried out in short stages and excessive grouting pressures should be avoided.

Fig.3

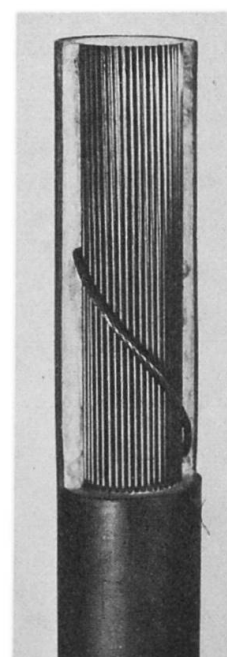
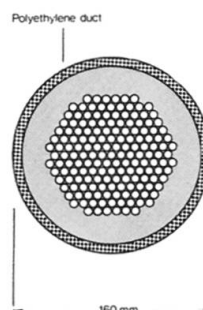




Fig.4 shows a model of a large cable containing 421 wires 7 mm dia. (ultimate tensile load 2600 t). This size of tendon has been designed for mooring systems for offshore oil platforms. The enclosing duct consists of a corrugated steel tube with an outer layer of polyethylene. Protection against corrosion is provided by a tar based filling compound.

Fig.4



## 2.2 Types of anchorages

Three different types of anchorages are available for use with the parallel-wire tendons described above. Fig.5 shows the BBRV-anchorage, well known from its application to prestressed concrete. All wires in a bundle are cut exactly to the same length and pass through pre-drilled holes in the anchorages. The BBRV button heads are then cold formed on each wire end and are brought to bear against the anchorage. Stressing of the tendon is carried out by means of a hydraulic jack acting on a pullrod screwed to the anchorage. When the required cable extension is reached, steel shims are inserted between the bearing plate and the anchorage, thus locking in the required prestressing force in the tendon.

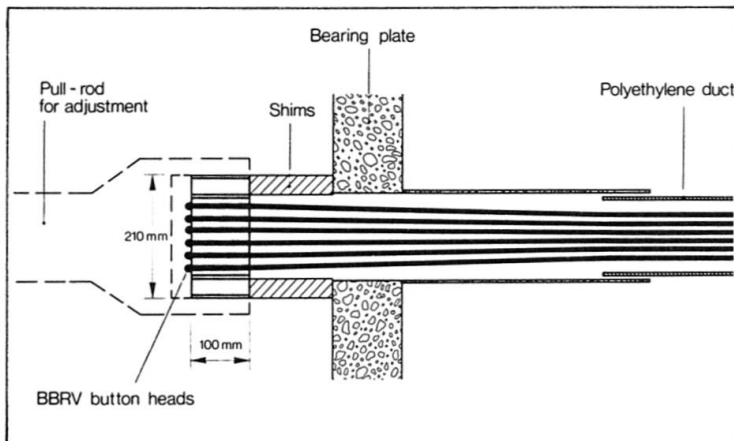


Fig.5

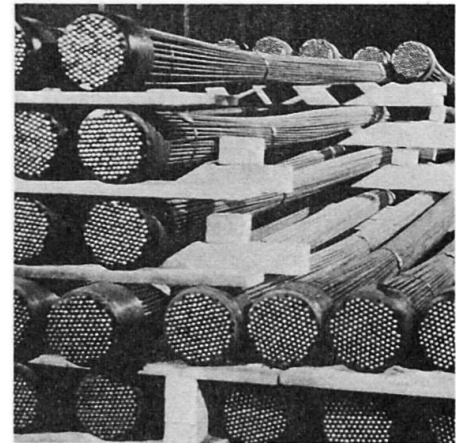


Fig.6

Fig.6 shows tendons containing 145 wires 7 mm dia. fitted with BBRV anchorages. The button heads are cold formed on the wire ends by means of a hydraulic button-heading machine (Fig.7). Extensive studies and experiments have led to the optimal forms for button heads shown in Fig.8. These button heads enable 100 % static anchorage efficiency to be consistently achieved using wires of even up to 200 kp/mm<sup>2</sup> tensile strength. The BBRV-anchorage is not adequate for use with parallel-wire tendons subject to high fatigue loading.

Fig.8

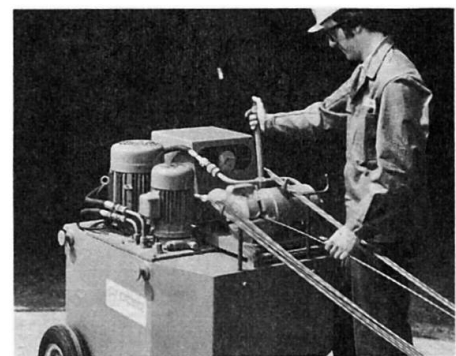
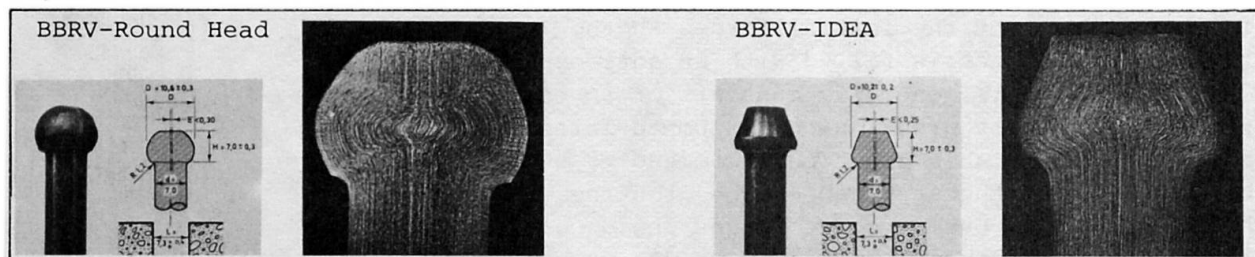


Fig.7



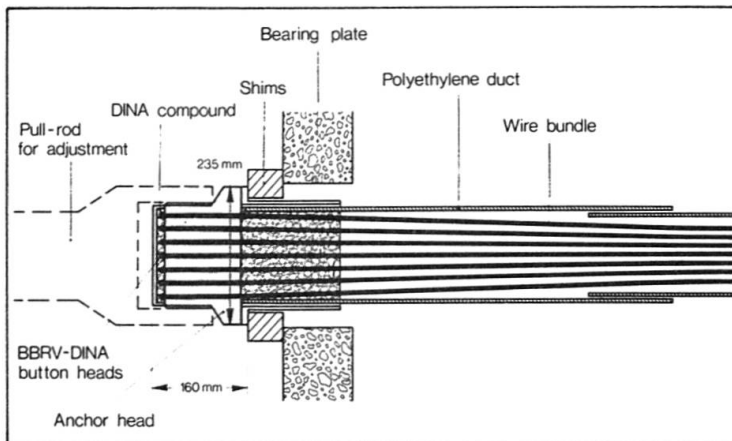


Fig.9

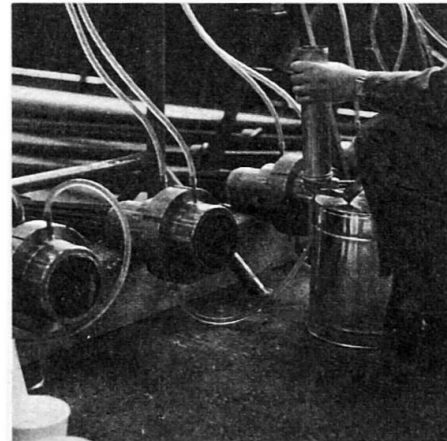


Fig.10

Fig.9 shows a longitudinal section through a BBRV-DINA anchorage which contains some special features aimed at providing a high fatigue resistance. The spaces between the wires, button heads and the anchorage are completely filled with a special epoxy compound. Fig.10 shows this operation being carried out in the works. This anchorage is suitable for use with tendons containing up to 250 wires 7 mm dia.

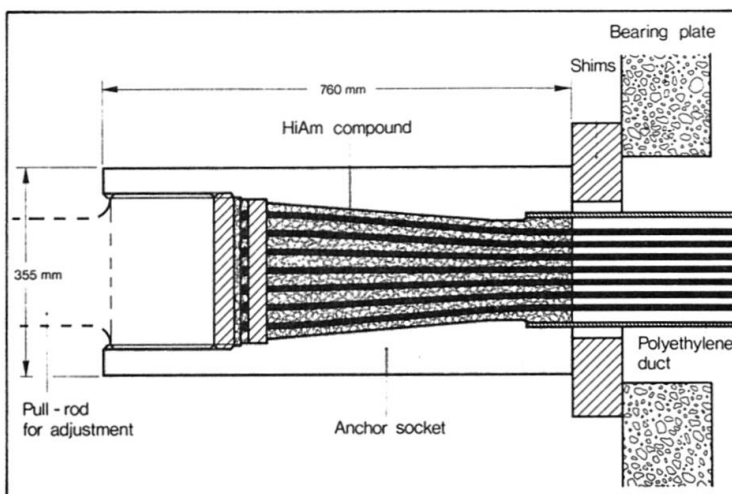


Fig.11

Fig.11 shows a longitudinal section through a HiAm anchorage. This form of anchorage is particularly suitable for use with large stay cables for bridges which are subject to high fatigue loading. This anchorage was developed jointly by the well known firm of engineers, Leonhardt und Andrä and BBR Ltd. [2]. The wires in the bundle are flared out slightly inside a steel casing and held against a steel plate by means of button heads at their ends. The conical space inside the steel casing is then filled with a mixture of steel pellets 1.5 - 2.0 mm diameter and an epoxy based resin. When a tendon anchored in this manner is loaded, arching action develops within the pellets in the resin mass inside the casing thus transmitting the load to the anchor. Fig.12 shows HiAm anchorages for tendons, each consisting of 295 wires 7 mm diameter. Two of the tendons are provided with adjustable rings to allow the tendon forces to be regulated.

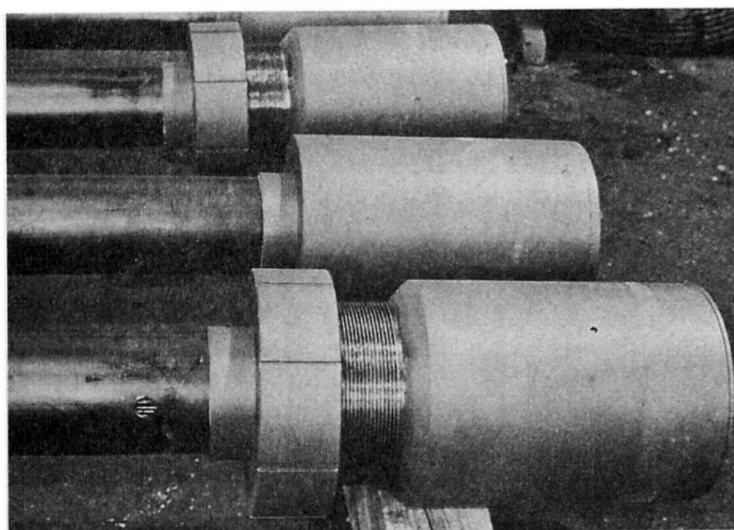


Fig.12



### 2.3 Sequence of fabrication and erection

The following photographs show the sequence of fabrication and erection for a large tendon with HiAm anchorages.

- Fig.13. View of the manufacturing area of Stahlton AG, Frick, Switzerland. The automatic cutting bench is seen on the right. Individual wires up to 250 m long can be cut exactly to the required length on this bench.
- Fig.14. The wires are coated with a film of anticorrosion fluid, pulled through a die to form a bundle and wrapped with a spiral strand. A polyethylene duct is drawn over the HiAm wire bundle. Duct joints are welded. The assembly of the HiAm anchorage takes place.
- Fig.15. Shows a tendon consisting of 295 wires 7 mm diameter with button heads and the steel plate. The steel casing and the die can also be seen on this slide.
- Fig.16. Filling the anchor casing with steel pellets and epoxy resin compound. Anchorage must be held vertical during this operation.

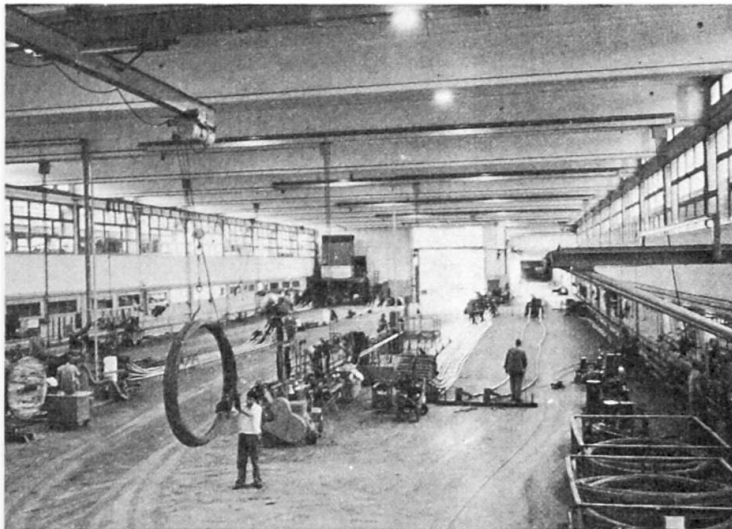


Fig.13

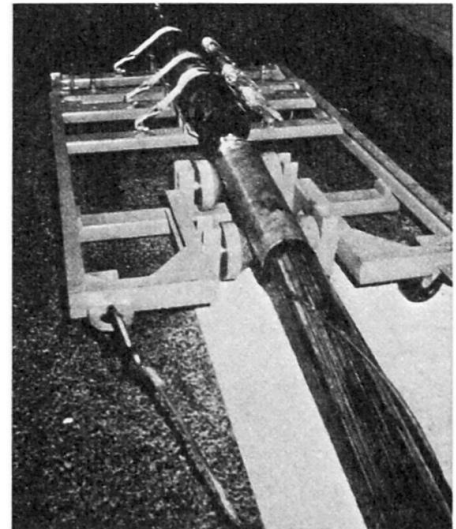


Fig.14

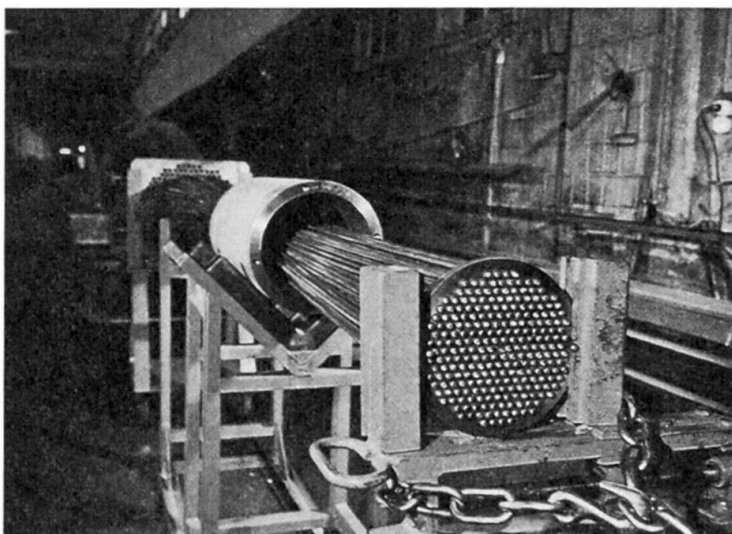


Fig.15

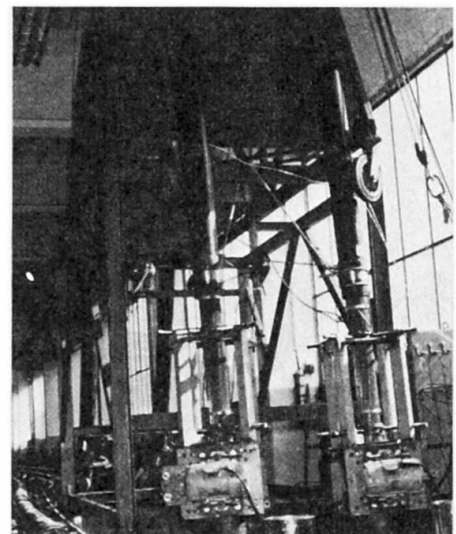


Fig.16

- Fig.17. Completed HiAm tendon being wound on to a bobbin.
- Fig.18. Bobbin with HiAm tendon ready for transport to site. Weight of bobbin with tendon 15 t.
- Fig.19. HiAm tendon during erection. Tendon being pulled up temporary ramp to top of pylon.

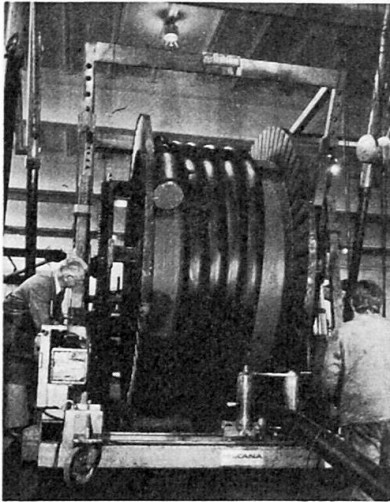


Fig.17

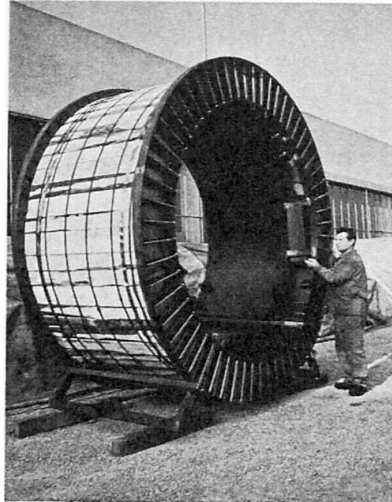


Fig.18



Fig.19

### 3. EXAMPLES OF COMPLETED STRUCTURES

The following photographs and figures show a range of building and bridge structures using inclined parallel-wire tendons.

- Fig.20. Roof over spectators' gallery at the Canberra Stadium (Australia), consisting of a light reinforced concrete slab supported by DINA tendons (7 per pylon).
- Fig.21. Lynne Bridge carrying double track rail traffic over the London Orbital Motorway M25. Prestressed concrete bridge deck across 2 spans of 55 m each. A total of 16 DINA tendons each consisting of 79 wires 7 mm dia. was used. [3]



Fig.20

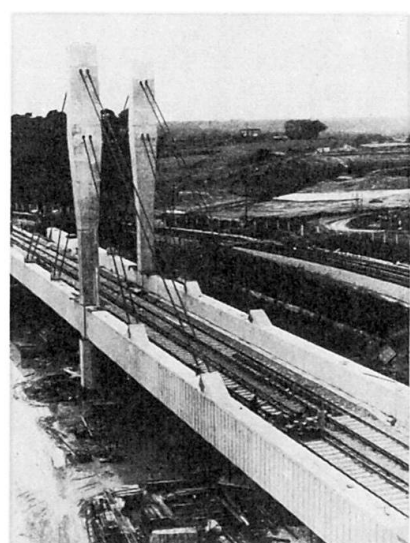


Fig.21



- Fig.22: Bridge across the river Reuss near Bremgarten (Switzerland). Continuous steel girder over main river opening of 66 m. Supported at third points by means of inclined parallel wire tendons.
- Fig.23. Bridge across R.Parana, Argentina. The main central opening has a span of 330 m. A total of 144 HiAm tendons with a maximum of 337 wires 7 mm dia. in some tendons was used. For further details see [4].

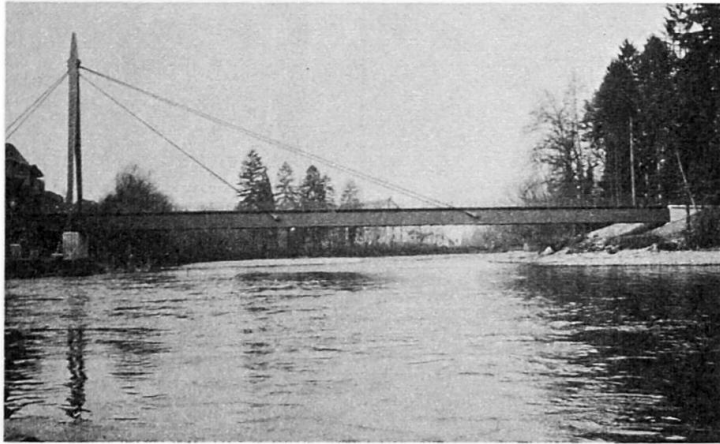


Fig.22



Fig.23

- Fig.24, 25, 26. Bridge across R.Save near Belgrade, Yugoslavia. The main central opening has a span of 254 metres. The bridge girders are of steel construction and the stay cables are clustered in groups of 4. A total of 64 HiAm tendons with a maximum of 290 wires 7 mm dia. in some tendons was used. When completed, the bridge will carry double track railway traffic. Due to the large stress fluctuation in the stay cables their fatigue resistance was a decisive criterion in the design. [5]

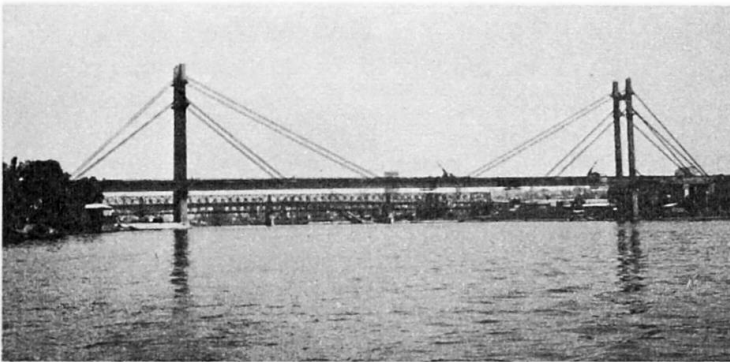


Fig.24

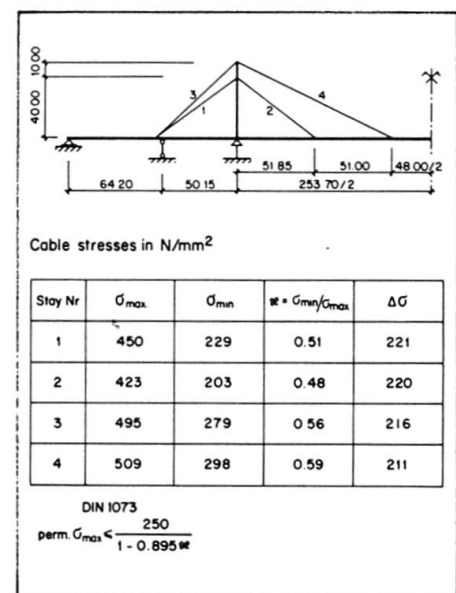


Fig.26

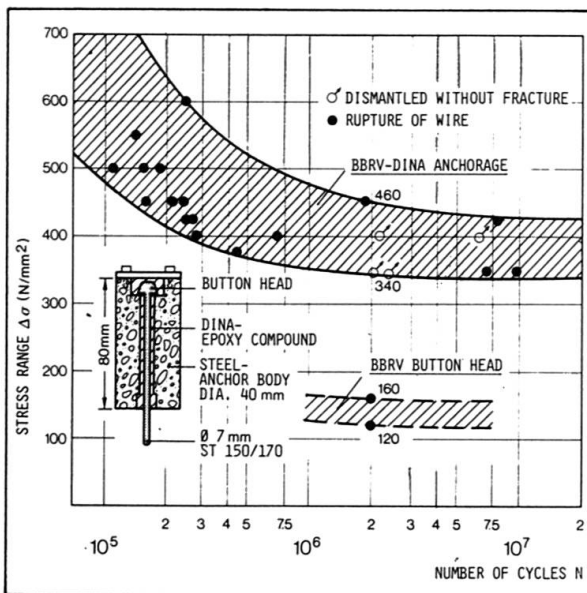
Fig.25

#### 4. FATIGUE AS A DESIGN CRITERION FOR TENDONS

##### 4.1 Fatigue tests on anchored tendons

Fig.27 shows the results of dynamic tensile tests on single-wire anchorages. The wire test specimens were anchored within a steel cylinder and subjected to a pulsating tensile load with a stress range  $\Delta\sigma = 2\sigma_a$  ( $\sigma_a$  = amplitude) at a value of upper stress  $\sigma_o = 0.65\beta_z$ . The number of load cycles  $N$  to failure was recorded. The results of these tests are plotted as a  $\Delta\sigma - N$  diagram - referred to as the Wöhler curve - in this figure.

Wire specimens anchored in the steel cylinder with button heads reached values of  $\Delta\sigma = 120 - 160 \text{ N/mm}^2$  for two million load cycles. These values are far below the  $\Delta\sigma$  value for the wire itself which is generally larger than  $350 \text{ N/mm}^2$ .



By completely filling up all hollow spaces between the wire, button head and the steel cylinder with a special epoxy compound it was found possible to improve the fatigue resistance values considerably. This figure also shows the result of tests on these modified anchorages and it can be seen that fatigue resistance values almost as high as that of the wire alone have been achieved.

Fig.27

Disposition of Bundle					Fatigue Test					Breaking Test after Fatigue	
TYPE	NUMBER OF WIRES	STEEL GRADE	AVERAGE TENSILE STRENGTH $\beta_z$	CALCULATED BREAKING LOAD $Z_u$	UPPER STRESS $\sigma_u$	AMPLITUDE $\Delta\sigma$	NUMBER OF CYCLES	NUMBER OF FAILURES	REDUCTION OF STEEL AREA	MEASURED BREAKING LOAD $Z_u'$	DAMAGE $\frac{Z_u - Z_u'}{Z_u}$
	mm	kp/mm <sup>2</sup>	kp/mm <sup>2</sup>	Mp	kp/mm <sup>2</sup>	kp/mm <sup>2</sup>	N	n	%	Mp	%
HiAm	295Ø7	140/160	169	1880	56	20	$2 \times 10^6$	3	1.0	1856	1.3
HiAm	295Ø7	140/160	178	1980	59	20	$2 \times 10^6$	1	0.3	1974	0.3
HiAm	19Ø7	150/170	179	128	60	20	$2 \times 10^6$	0	0	128	0
DINA	102Ø7	150/170	179	688.6	60	20	$2 \times 10^6$	0	0	688.6	0
DINA	55Ø7	150/170	175	363	110	25	$2 \times 10^6$	0	0	363	0
Remarks: - CALCULATED BREAKING LOAD $Z_u \approx 0.98 \times \beta_z \times F_s$ ( $F_s$ = STEEL AREA) - ELONGATION OF BUNDLE (WHEN $\sigma < 0.7 \times \beta_z$ YOUNG'S MODULUS OF WIRE AND BUNDLE) = $20'500 \text{ kp/mm}^2$ - LENGTH OF TESTED BUNDLES $\approx 4.0 - 4.5 \text{ m}$ - ALL FAILURES OF WIRES ARE LOCATED BEYOND ANCHORS											

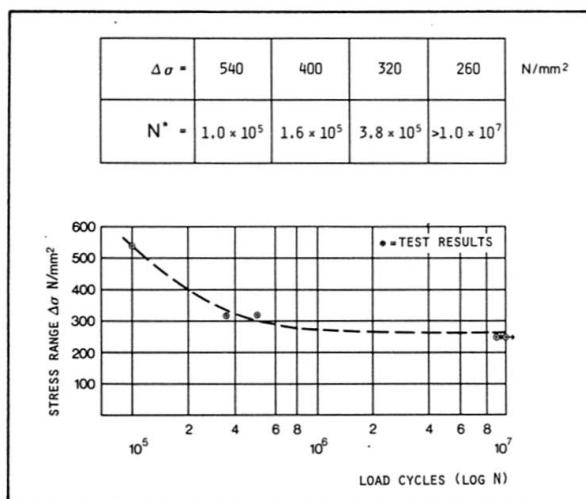
Table 1 shows the results of fatigue tests on parallel wire tendons fitted with HiAm or DINA anchorages. The tendons were subjected to dynamic loading with stress ranges  $\Delta\sigma = 20$  and  $25 \text{ kp/mm}^2$  for up to 2 million load cycles. In conclu-



sion, these tendons were subjected to a static rupture test. The load at rupture,  $F_{Rupt.}$ , was then compared with the theoretical ultimate tendon load  $F_{U.T.S.}$ . By this means it was possible to assess the reduction in static ultimate tensile strength of the tendon caused by the preceding fatigue loading. This is often referred to as fatigue damage. The results of these tests show clearly that the damage caused by the fatigue loads was extremely minimal. It is also worthy of note that, during the static rupture tests, wire failure occurred in zones lying outside the anchorages. [6]

Fig.28 shows the results of fatigue tests on a series of 6 identical tendons fitted with HiAm anchorages. Each tendon was subjected to a different dynamic stress range  $\Delta\sigma = 540, 400, 320$  or  $260 \text{ N/mm}^2$ . The test results have been evaluated for each of the above  $\Delta\sigma$  values to determine the value of  $N^*$  load cycles at the end of which the remaining static rupture load of the tendon,  $F_{Rupt.}$ , is greater than 90 % of its theoretical ultimate value,  $F_{U.T.S.}$ .

In all static and dynamic tensile tests on tendons fitted with HiAm or DINA anchorages the wire failure occurred in the free length of the tendon. The anchorages did not reduce either the static or the dynamic tensile strength of the tendons. These tendon properties are therefore primarily governed by the corresponding properties of the wire bundle alone. In order therefore to determine the load behaviour of the tendon it is essential to know the mechanical properties of the wire used to a reasonable accuracy.



#### Test Method

- Series of 6 tendons 19 wires dia. 7 mm, ST 1500/1700 HiAm anchorage, Length 6.0 m
- Fatigue loading with constant stress range  $\Delta\sigma = 540; 400; 320$  (2 tendons); 260 (2 tendons)  $\text{N/mm}^2$
- Lower stress kept constant at:  $\sigma_u = 350 \text{ N/mm}^2$
- Number of load cycles with  $\Delta\sigma$ :  $N^*$

Fig.28

#### 4.2 Testing of wires

In order to assess any material characteristics such as tensile strength or the fatigue resistance of a collection of a large number of wires in a tendon, it is important that great care is exercised in the method of testing employed and that statistical methods are used in the evaluation of results.

Fig.29 shows a summary of static tensile test results relating to a delivery of 7 mm dia. wire. 1800 specimens were tested and showed an average tensile strength of  $173.3 \text{ kp/mm}^2$  with a standard deviation of only  $\pm 3.3 \text{ kp/mm}^2$ . The yield limit and elongation at rupture values for 361 specimens also show a relatively small value of standard deviation. One can safely assume from this that the wire delivered is uniform in quality.

Particular attention must be paid to the choice of a systematic method of testing for determining the fatigue resistance of the wires because of the large scatter of test results encountered.

Fig.30 shows the well-known and popular method of plotting the results of a small number of fatigue tests in the form of a "Smith Diagram". For a given value of average stress  $\sigma_m$  the value of stress range  $\Delta\sigma = 2\sigma_a$  which can be endured by the

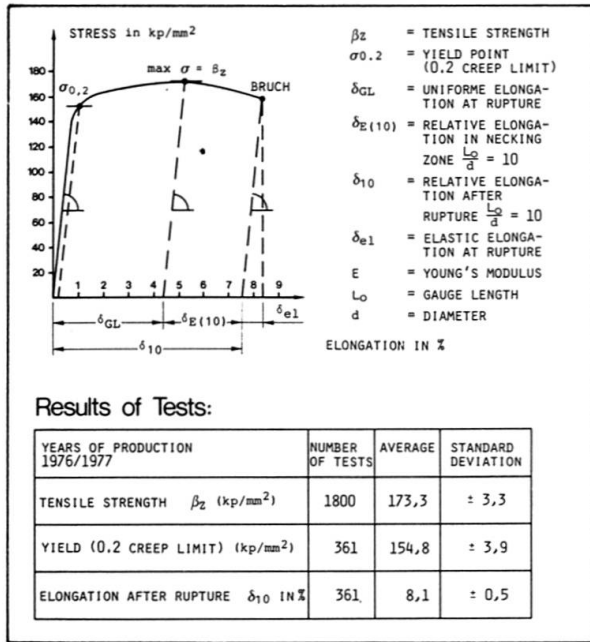


Fig. 29

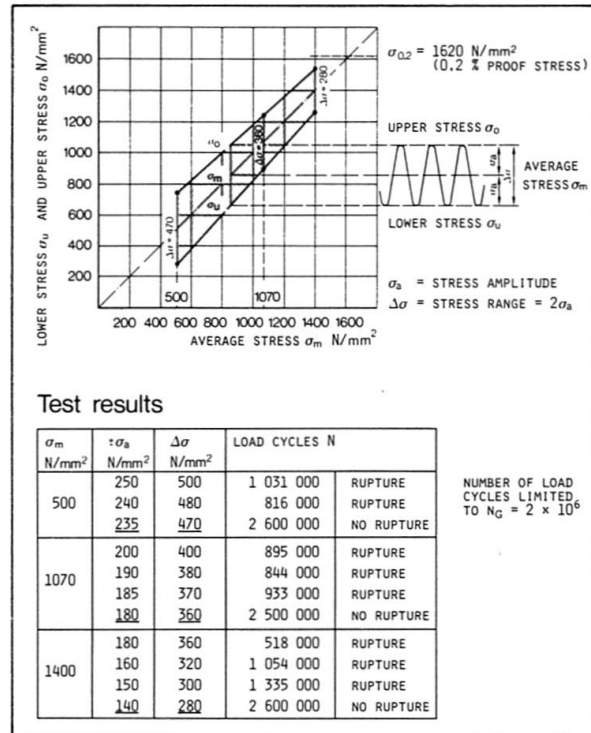


Fig. 30

wire for 2 million load cycles is determined. This procedure is repeated for three different values of average stress  $\sigma_m$  and the results can then be plotted as a Smith diagram for fatigue strength. It is seen from this diagram that for a value of upper stress  $\sigma_o < 0.50\beta_z = 850 \text{ N/mm}^2$ , the stress range  $\Delta\sigma$  withstood by the wire is almost independent of the values of upper or average stress. It should be noted that this diagram has been drawn using the results of a small number of tests and cannot therefore reflect the large scatter which in reality occurs in the values of fatigue resistance of wires.

A more comprehensive method of determining the fatigue resistance of the wires is to organize the testing so as to obtain a "complete random block" [7]. As shown in Fig. 31 this has been achieved by choosing 5 equally spaced values of stress range  $\Delta\sigma = 350, 400, 500$  and  $550 \text{ N/mm}^2$ , and 42 specimens to be tested at each stress range. Testing was done up to a maximum value of two million load cycles. It was assumed that practically infinite fatigue life is reached when a specimen endures the applied dynamic load for two million load cycles. Specimens which fail below this value of N are said to be in the finite fatigue life range. The values of N at which the specimens ruptured during the test are marked by the vertical dashes in Fig. 31. The numerical values against the circles give the number of specimens which did not rupture during the test duration over  $N_G = 2 \cdot 10^6$  load cycles.

The total number of 210 specimens tested was taken from 116 wire coils (weight of each coil about 450 kg) and may therefore be considered to be randomly chosen to represent the collective.

The test results can be interpreted statistically to enable a set of Wöhler curves with different fractile values to be drawn [8].

The fractiles for the fatigue strength at two million load cycles are calculated using the observed frequency of ruptured specimens  $r/n$  for each stress range. However, Weibull has suggested [9] that the following corrected value of probability of rupture  $P_r$  should be used to cover the two extreme ends of the probability range, viz.,

$$P_r = \frac{3r - 1}{3n + 1} \cdot 100$$



If these values of  $P_r$  are plotted as ordinates against  $\Delta\sigma$  as abscissae, an S-shaped curve results which is typical for normal distributions. Here, in Fig.31, the  $P_r$  values are plotted to an arithmetic probability scale, and the normal distribution is evident from the resulting straight line graph. The 5 %, 16 % and 50 % fractile values of infinite fatigue life and the standard deviation may now be read off this diagram.

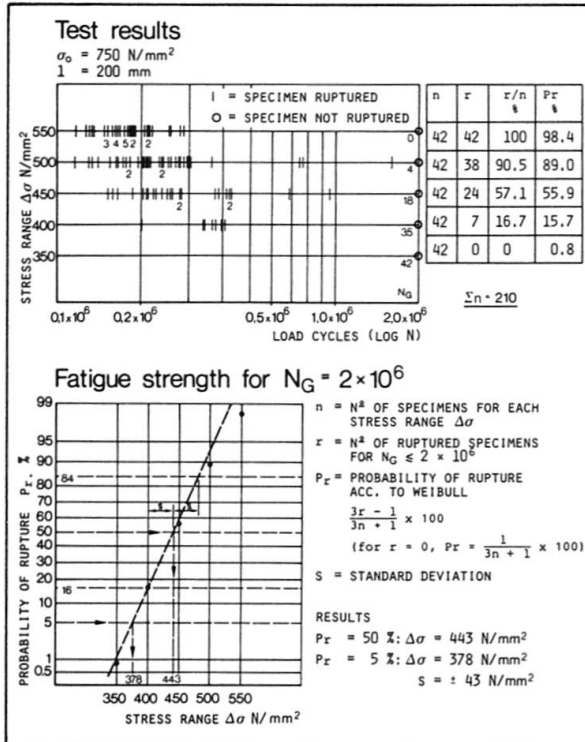


Fig.31

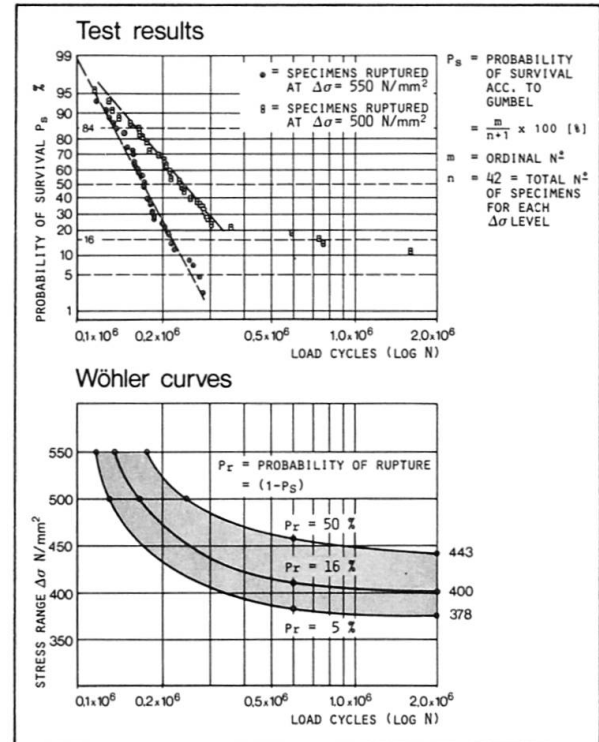


Fig.32

The fractiles for the fatigue strength  $\Delta\sigma$  in the finite life range (i.e.  $\Delta\sigma = 550 \text{ N/mm}^2$  and  $500 \text{ N/mm}^2$ ) are next determined [10]. For any given stress range, the values of  $N$  at failure for each of the specimens tested ( $n = 42$  in our case) are recorded in a vertical list beginning with the largest value of  $N$ . Each specimen is allocated an "ordinal number  $m$ " beginning with  $m = 1$  for the specimen with the largest value of  $N$ . The value of  $m$  thus specifies the number of specimens which have survived a given number of load cycles  $N$  for the stress range being considered. The value of  $\frac{m}{n} \cdot 100$  for a specimen gives the cumulative frequency with which the specimen can survive  $N$  load cycles. Gumbel has suggested the following formula [11] for calculating the probability of survival  $P_s$  for a specimen (Fig.32).

$$P_s = \frac{m}{n+1} \cdot 100$$

and that these  $P_s$  values follow a log.-normal distribution. The  $P_s$  values are therefore plotted against  $N$  on arithmetic probability paper in Fig.32 using a log. scale for  $N$ . The plotted points are seen to lie almost on a line. The 95 %, 84 % and 50 % fractiles of  $P_s$  can be read off this figure. It is obvious that these are also the 5 %, 16 % and 50 % fractiles respectively of the probability of rupture  $P_r$ , since  $P_r = (1 - P_s)$ .

The fractiles so far determined both for the infinite and finite life range of the specimens can now be plotted as a  $\Delta\sigma - N$  diagram to produce Wöhler curves for  $P_r = 5\%$ ,  $16\%$  and  $50\%$  (Fig.32). Ideally, it would be desirable to have a Wöhler curve for  $P_r \approx 0$  which would define the lowest fatigue strength for the collective being tested. However, the relatively simple statistical method de-

scribed here is unsuitable for the evaluation of this limiting case of  $P_r$ . The group of curves in Fig.32 shows clearly that the scatter of fatigue values is quite large even though the static tensile strength of the wire was found to be reasonably uniform. It cannot be overemphasized that a reliable assessment of the range of scatter in the fatigue strength of steel wires is only possible through carefully planned and comprehensive testing.

#### 4.3 Design assumptions for fatigue calculations

The determination of the permissible stress range for tendons with HiAm and DINA anchorages should be based on the Wöhler curves of the wires used in the tendons. Generally the 5 % fractile value is chosen as the basis. In Fig.33 the 5 % fractile Wöhler curve is shown and is labelled as the intrinsic fatigue strength of the wire,  $\Delta\sigma_{wire}$ , since it specifies the fatigue behaviour of the basic material i.e. wire, to a reasonable accuracy [12]. The choice of the 5 % Wöhler curve as the basis curve also practically eliminates the effects of test specimen lengths on the test results, since this 5 % fractile value lies very close to the lowest fatigue strength ( $P_r \approx 0$ ) of the basic material. Should the 50 % fractile Wöhler curve, or in other words, the mean value be used it will be found that longer specimen lengths yield a mean value which is smaller than that obtained with short specimen lengths.

The curve for the permissible stress range in the anchored tendon can be derived from the basis curve mentioned above by introducing partial reduction factors  $\gamma_1$  and  $\gamma_2$ , so that

$$\text{perm } \Delta\sigma_{\text{Tendon}} = \frac{1}{\gamma_1 \cdot \gamma_2} \Delta\sigma_{\text{Wire}}$$

The transition from the lowest fatigue strength of the basic wire to the fatigue strength of the anchored tendon installed in the structure is approximated by assuming a factor  $\gamma_1 = 1.3$ . This factor should also account for other influences

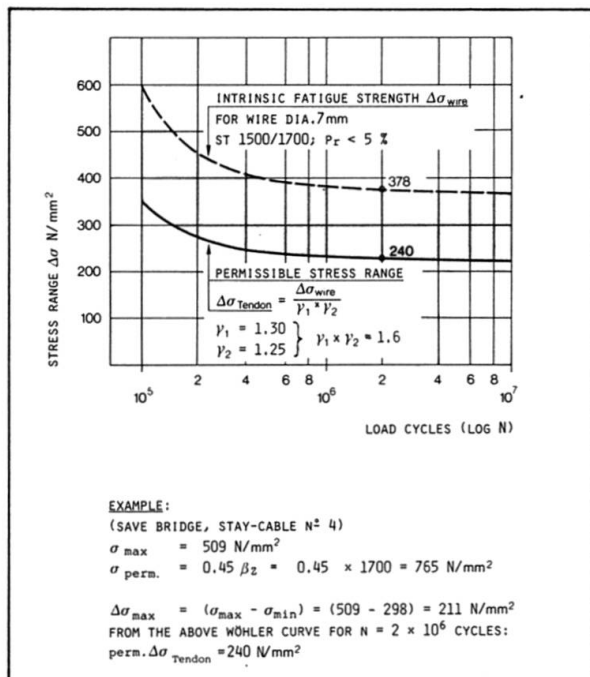


Fig. 33

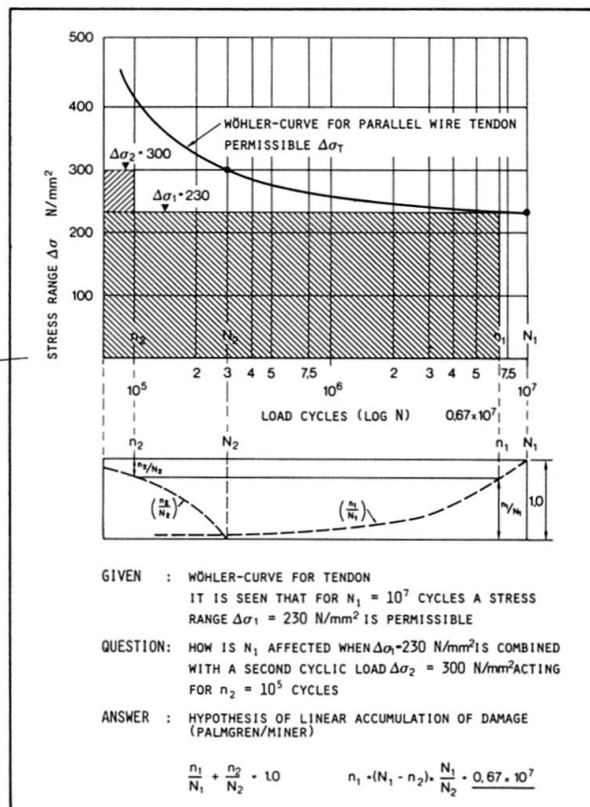


Fig. 34



such as minor random surface defects in wire, manufacturing tolerances, secondary effects in anchorage zones etc. An additional margin of safety is introduced by choosing a value of 1.25 for the factor  $\gamma_2$ . With these assumptions the permissible stress range for the anchored tendon is given by

$$\text{perm } \Delta\sigma_{\text{Tendon}} = \frac{\Delta\sigma_{\text{Wire}}}{1.6}$$

Extensive tests on anchored tendons yield results which show that the above assumptions for the permissible stress range in the tendon are indeed safe. It is to be noted that after  $N$  load cycles with a stress range of  $\text{perm } \Delta\sigma_{\text{Tendon}}$  the fatigue damage to the tendon will be always less than 5 %, i.e. the static rupture load of the tendon after the dynamic loading will be at least 95 % of its theoretical rupture load.

All tests so far have clearly shown that the level of upper stress  $\sigma_0$  in the tendon has only a very small influence on the value of stress range endured by the tendon, provided  $\sigma_0 < 0.5\beta_z$ . In designing for fatigue, therefore, only the applied stress range  $\Delta\sigma$  and the number of load cycles  $N$  are the principal factors to be considered. This Delta Sigma concept has found acceptance in some American and European codes of practice [13], [14].

The main design steps for a tendon in a cable stayed structure can now be summed up as follows (See example in Fig.33)

for static loading:

check that the maximum stress in the tendon under total load

$$\sigma_{\text{max}} < 0.45\beta_z$$

$\beta_z$  = nominal tensile strength of the wires used in tendon

for fatigue loading:

check that max. stress range  $\Delta\sigma_{\text{max}}$  in the tendon under fatigue loading  $\leq$  permissible  $\Delta\sigma_{\text{Tendon}}$  of the anchored tendon for  $N$  load cycles.

In this condition the value of  $\Delta\sigma_{\text{max}}$  is to be calculated only for the fatigue load component of the total live load. This component varies with the type of structure being considered. For example, DIN 1073 specifies the fatigue load component to be 50 % of the total live load for road bridges and 100 % for railway bridges [15].

The value of  $N$  in the above condition will be determined by the intensity of live load traffic and the planned life of the structure.

An additional problem sometimes arises in practice in that a tendon is subjected to dynamic loads with differing stress ranges. Fig.34 shows a simple example of such a loading and the solution using the Palmgren-Miner rule for the linear accumulation of damage [16], [17].

Conversion of units:

$$1 \text{ kp/mm}^2 = 10 \text{ N/mm}^2 \quad 1 \text{ kp} = 10 \text{ N} \quad 1 \text{ t} = 10 \text{ kN}$$

#### REFERENCES

- [1] Leonhardt F.: Latest developments for cable-stayed bridges for long spans. Byggningsstatistiske Meddelelser, Vol.45, No.4, 1974
- [2] Andrä W., Saul R.: Versuche mit Bündeln aus parallelen Drähten und Litzen für die Nordbrücke Mannheim-Ludwigshafen und das Zeltdach in München. Die Bautechnik 51 (1974), Hefte 9, 10 und 11

- [3] All-concrete cable-stayed railway bridge. Concrete International, Design & Construction, December 1979, Vol.1, No.12
- [4] Leonhardt F., Zellner W., Saul R.: Zwei Schrägkabelbrücken für Eisenbahn- und Strassenverkehr über den Rio Paraná (Argentinien). Der Stahlbau 48 (1979), Heft 8
- [5] Hajdin N., Jevtovic Lj.: Eisenbahnschrägseilbrücke über die Save in Belgrad. Der Stahlbau 47 (1978), Heft 4
- [5] Andrá W., Zellner W.: Zugglieder aus Paralleldrahtbündeln und ihre Verankerung bei hoher Dauerschwellbelastung. Die Bautechnik 46 (1969), Hefte 8 und 9
- [7] Dengel D.: Einige grundlegende Gesichtspunkte für die Planung und Auswertung von Dauerschwingversuchen. Materialprüfung 13 (1971), Heft 5
- [8] Maennig W.W.: Untersuchungen zur Planung und Auswertung von Dauerschwingversuchen an Stahl in den Bereichen der Zeit- und der Dauerfestigkeit. Fortschr.-Ber. VDI-Z, Reihe 5, Nr.5. Düsseldorf: VDI-Verlag, August 1967
- [9] Weibull W.: A statistical representation of fatigue failures in solids. Transactions of the Royal Inst. of Technology Stockholm, Nr.27 (1949)
- [10] Gassner E.: Zur Aussagefähigkeit von Ein- und Mehrstufen-Schwingversuchen. Materialprüfung 2 (1960), Heft 4
- [11] Gumbel E.J.: Statistische Theorie der Ermüdungserscheinungen bei Metallen. Mitt.-Bl. Math. Statistik 8 (1956), Nr.2
- [12] Duggan T.V., Byrne J.: Fatigue as a design criterion. The Macmillan Press Ltd., 1977 London
- [13] Hirt M.A., Dr.: Neue Erkenntnisse auf dem Gebiet der Ermüdung und deren Berücksichtigung bei der Bemessung von Eisenbahnbrücken. Der Bauingenieur 52 (1977), S.255-262
- [14] SIA Norm 161: Stahlbauten, Ausgabe 1979
- [15] DIN 1073: Stählerne Strassenbrücken. Ausgabe Juli 1974
- [16] Palmgren A.: Die Lebensdauer von Kugellagern. VDI-Z 68 (1924), Nr.14, S.339-341
- [17] Miner M.A.: Cumulative damage in fatigue. Proc. Amer. Soc. Mech. Engrs. Metals 67 (1945), S.A. 159-164
- [18] Borges J.F.: Safety Concepts for Non-Repeated and Repeated Loadings. Introd. Report, IABSE Symposium on Resistance and Ultimate Deformability of Structures Acted on by Well Defined Repeated Loads. Lisboa 1973
- [19] Gabriel K.: Anwendungen von statistischen Methoden und Wahrscheinlichkeitsbetrachtungen auf das Verhalten von Bündeln und Seilen als Zugglieder aus vielen und langen Drähten. Vorberichte 2.Internationales Symposium Stuttgart 1979 über weitgespannte Flächentragwerke